

CHAPTER 98

TIDAL INLET FLOW DYNAMICS AND SEDIMENT MOVEMENT

J. L. Machemehl, N. E. Bird and A. N. Chambers
Center for Marine and Coastal Studies
North Carolina State University
Raleigh, North Carolina 27607

ABSTRACT

A numerical simulation model for the computation of tidal and fresh water flow exchange through a coastal inlet (developed by Amein¹) was modified and calibrated with field data (current, water surface elevation and bottom topography) for Lockwoods Folly Inlet, North Carolina. The calibrated model was then used to predict the changes in the flow regimes brought about by natural and manmade changes such as storms and dredging, respectively, and to predict the changes in flow regimes caused by the Lockwoods Folly River.

A generalized hypothesis of the patterns of sediment through and bypassing the inlet were formulated from an evaluation of the flow data and from an analysis of the orientation and structure of the bedforms observed in the inlet and on the offshore bar. The bedforms were analysed in the field and from an uncontrolled mosaic made from multi-spectral aerial photographs. Confirmation and refinement of the transport rates and movement patterns during ebb tide were made by introducing 454 kilograms (1000 lbs.) of fluorescent tracer sand in two colors into the inlet channels. The sediment movement through the inlet was established and correlated with the numerical simulation model. Confirmation and refinement of the transport rates and movement patterns during flood tide were made by introducing 680 kilograms (1,500 lbs.) of fluorescent tracer sand in three colors into the surf zone on the updrift beach and on the offshore bar. The sediment movement indicated the existence of bar bypassing (which was the dominant bypassing mechanism) and tidal flow bypassing. The bypassing mechanism of the inlet was found to agree with other atlantic coast inlets.

When used in conjunction with an analysis of bedform and tracer sand data the numerical simulation model was found to be a valid method for monitoring the high energy inlet environment.

INTRODUCTION

Description of the Study Area

Lockwoods Folly Inlet is approximately 10 miles west of the Cape Fear River and 9 miles east of Shallotte Inlet in Brunswick County, North Carolina. Holdens Beach borders the Inlet on the west while

Long Beach borders the Inlet on the east as shown in Figure 1. The beaches are almost east-west in direction. Holdens Beach is approximately 13,400 meters (44,900 ft.) long and has an average width of 490 meters (1600 ft.) while Long Beach is approximately 14,000 meters (46,000 ft.) long and has an average width of 400 meters (1300 ft.). Both the eastern end of Holdens Beach and the western end of Long Beach have been the victim of extensive and severe erosion. The Corps of Engineers² has stated that the eastern 1,800 meters (6,000 ft.) of Holdens Beach has experienced the highest rate of shoreline erosion in Brunswick County. Shoreline positions in the vicinity of the Inlet are shown in Figure 1.

The Atlantic Intracoastal Waterway (AIWW) separates the beaches from the mainland. The Lockwoods Folly River enters the AIWW 2100 meters (6900 ft.) east of the Inlet. In 1672 the Inlet was aligned with the Lockwoods Folly River.

Meterological and Oceanographical Data

On an annual basis the winds blow almost equally onshore and offshore with winds from the east occurring less frequently. During the period of this study the predominant wind was south to southeast at an average speed of 1.9 meters per second (3.7 knots). Wave height and direction data were available from the Corps of Engineers. The waves observed had a period of less than 9 seconds and a height of less than 5 ft. Unusual conditions during the study included a period of squalls and several days of storms.

The mean tidal range at Lockwoods Folly Inlet was 1.3 meters (4.2 ft.). The spring tidal range is 1.5 meters (4.8 ft.). The tides are semi-diurnal. The current velocities in the Inlet channel ranged from 129 to 160 cm/sec. (2.0 to 2.5 knots).

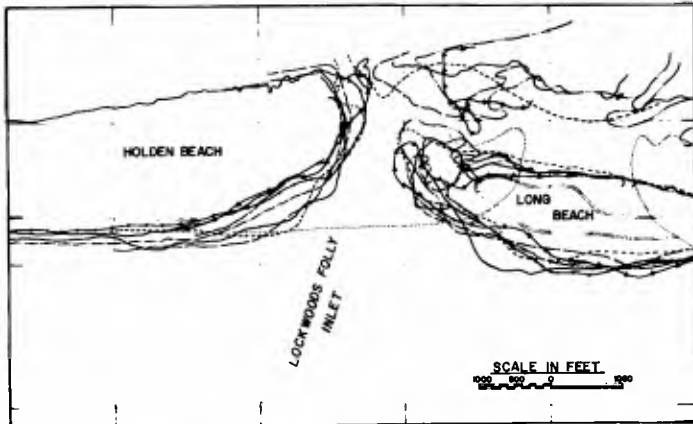
Objectives of Study

Lockwoods Folly Inlet is of particular interest as a study area. The Inlet is included in a proposed Corps of Engineers project for erosion control and hurricane protection of adjacent beaches. The Inlet is very active with strong tidal currents and shoaling sand bars. Wave energy is frequently concentrated near the Inlet due to refraction around the offshore sand bar which tends to aggravate the erosion.

The objectives of this study were:

- (1) To adapt Amein's numerical model to the Inlet,
- (2) To develop a generalized sediment movement pattern for the Inlet, and
- (3) To evaluate the natural bypassing system at the Inlet.

INLET FLOW DYNAMICS



LEGEND

DATE	HIGH WATER SHORELINE
1859
1923	-----
1934	-----
1943	-----
1954	-----
1961	-----
1963	-----
1970	-----
1972	-----

FIGURE 1. Historic Shoreline Positions for Lockwoods Folly Inlet, North Carolina.

Numerical Simulation Model

Flow Computations. Amein's¹ numerical simulation model was modified and adapted to Lockwoods Folly Inlet. The numerical simulation model is based on the equations of unsteady flow with an implicit method for numerical simulation of the flow equations. A system of 28 nonlinear equations were solved using the generalized Newton iteration method.

The equations of unsteady flow are based on the conservation of mass and momentum. For the flow between Section 1-1 and 2-2 as shown in Figure 2, the equations can be written:

$$\frac{\partial Q}{\partial x} + \frac{\partial A}{\partial t} - q = 0 \dots \dots \dots (1)$$

And

$$\frac{1}{A} \frac{\partial Q}{\partial t} + \frac{V}{A} \frac{\partial Q}{\partial x} + V \frac{\partial V}{\partial x} = -g \frac{\partial y}{\partial x} -g \frac{\partial z}{\partial x} -g S_f \dots \dots \dots (2)$$

Where Q is the discharge, q is the point discharge, V is the velocity, g is the acceleration of gravity, y is the depth of flow and s_f is the friction slope.

A non-uniform rectangular grid in the x and t plane as shown in Figure 3 was used to simulate Equations 1 and 2 for numerical solution. The differential equation were simulated for a finite time Δt and a finite distance Δx . Equation 1 is simulated by

$$\frac{Q_{i+1}^{j+1} - Q_i^{j+1}}{\Delta x} + \frac{\bar{A}_{i+1/2}^{j+1} - \bar{A}_{i+1/2}^j}{\Delta t} - q_{i+1/2}^{j+1} = 0 \dots \dots \dots (3)$$

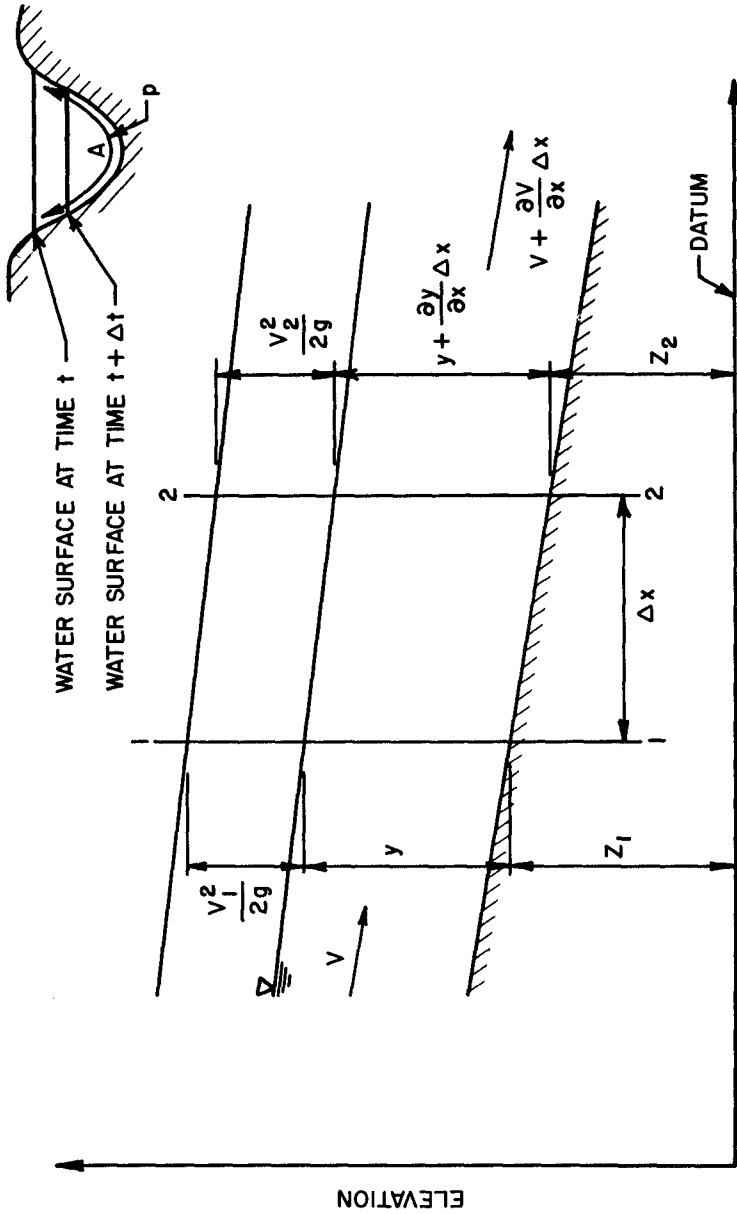
where

$$\bar{A}_{i+1/2} = \int_{x_i}^{x_{i+1}} A(x) \Delta x \dots \dots \dots (4)$$

$\bar{A}_{i+1/2}$ is approximated by $\frac{1}{2} (A_i + A_{i+1})$

Equation 2 is simulated by

$$\frac{1}{A_{i+1/2}^{j+1}} \frac{Q_{i+1/2}^{j+1} - Q_{i+1/2}^j}{\Delta t} + \frac{1}{(\bar{A}_{i+1/2}^j)^2} \frac{1}{2\Delta x} \left\{ (Q_{i+1}^{j+1})^2 - (Q_i^{j+1})^2 \right\} +$$



LONGITUDINAL SECTION
 Definition Sketch for Open Channel Flow.

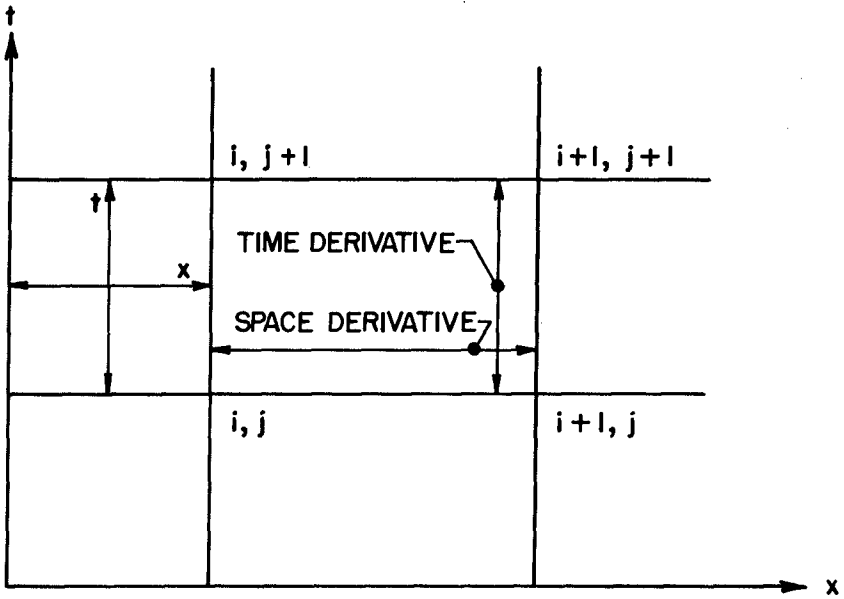


FIGURE 3. Definition Sketch for a Network of Points on the x, t Plane.

$$\frac{1}{2\Delta x} \left\{ \left(\frac{Q_{i+1}^{j+1}}{A_{i+1}^{j+1}} \right)^2 - \left(\frac{Q_i^{j+1}}{A_i^{j+1}} \right)^2 \right\} + g \left[\frac{(y_{i+1}^{j+1} + z_{i+1}) - (y_i^{j+1} - z_i)}{\Delta x} \right] + \bar{S}_{f_{i+1}}^{j+1} = 0 \dots \dots \dots (5)$$

where

$$\bar{Q}_{i+1/2}^{j+1} = \frac{1}{\Delta x} \int_{x_i}^{x_{i+1}} Q(x, t) dx \dots \dots \dots (6)$$

and

$$\bar{S}_{f_{i+1/2}}^{j+1} = \frac{1}{\Delta x} \int_{x_i}^{x_{i+1}} S_f(x, t) dx \dots \dots \dots (7)$$

or

$$\bar{Q}_{i+1/2}^{j+1} = \frac{1}{2} \left\{ Q_{i+1}^{j+1} + Q_i^{j+1} \right\} \dots \dots \dots (8)$$

and

$$\bar{S}_{f_{i+1/2}}^{j+1} = \frac{1}{2} \left\{ S_{f_{i+1}}^{j+1} + S_{f_i}^{j+1} \right\} \dots \dots \dots (9)$$

The approximations of \bar{A} , \bar{Q} and \bar{S}_f are based on a linear assumption, and if Δx is sufficiently small the result would be valid.

The unknown variables in the simulation equations are the ones with the superscripts $(j + 1)$. The independent unknowns are the values of discharge and stage at grid points $(i, j+1)$ and $(i+1, j+1)$. For an inlet system the part of equations with four unknowns can be evaluated because the additional equations obtained from the boundary conditions and channel junctions will result in the same number of equations as there are unknowns.

Application: to Lockwoods Folly Inlet

For problem purposes the inlet was represented by 14 stations as shown in Figure 4. The channel system was divided into five channels with two junctions. The channel sections are:

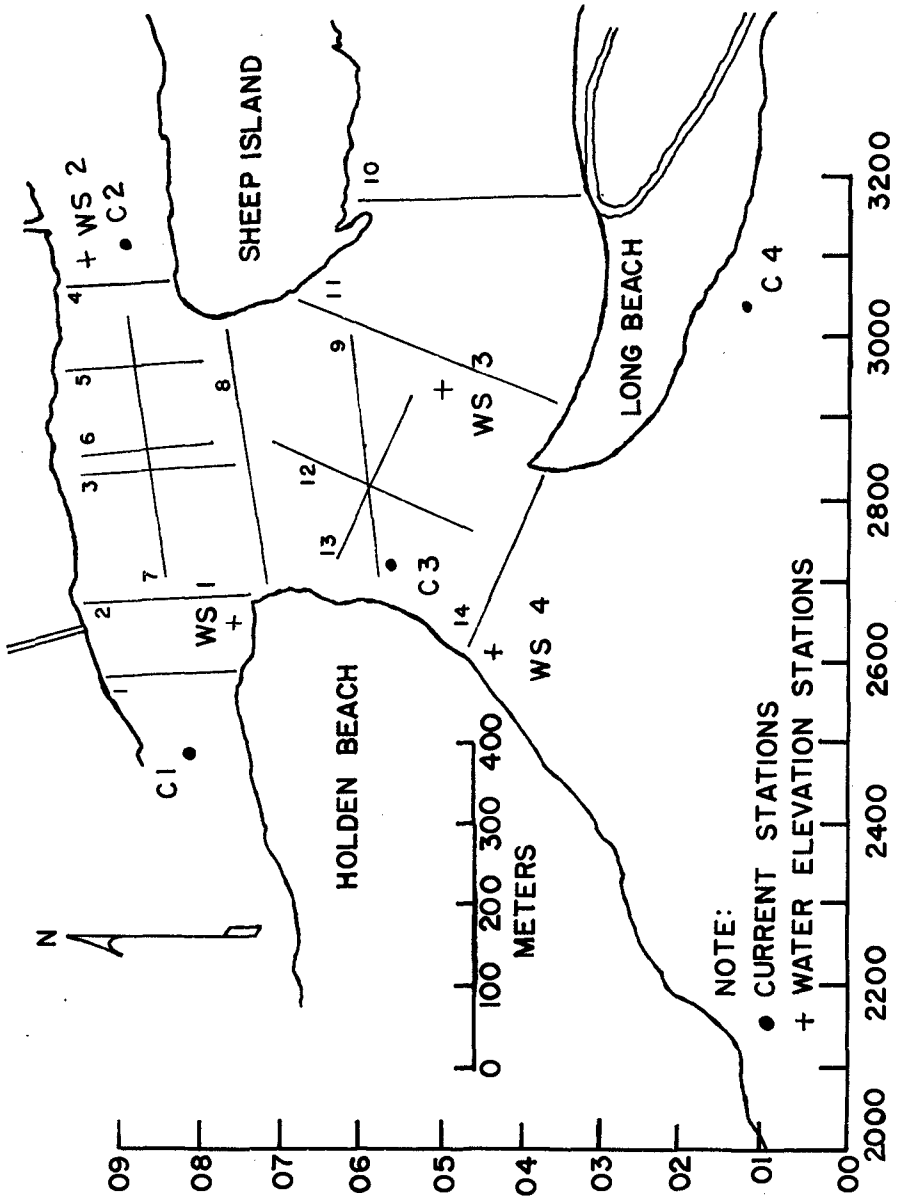


FIGURE 4. Flow Stations.

- 1, 2, 3
- 4, 5, 6
- 7, 8, 9
- 10, 11, 12
- 13, 14

The junctions are:

- 3, 6, 7
- 9, 12, 13

The value of x is taken as zero at junction 9, 12, 13 and increases to seaward. The flow during an ebb tide is in the positive x direction.

The simulated equations of conservation and momentum, Equation 3 and Equation 5 are abbreviated by:

$$F(Q_i, Q_{i+1}, y_i, y_{i+1}) = 0 \dots \dots \dots (10)$$

$$G(Q_i, Q_{i+1}, y_i, y_{i+1}) = 0 \dots \dots \dots (11)$$

$Q_i, Q_{i+1}, y_i, y_{i+1}$ are values of discharge and stage at time $j+1$. Since all unknown quantities are at time $j+1$ that superscript has been omitted. Equations 10 and 11 can be written for each channel section as follows:

Section 1, 2, 3

$$F(Q_1, Q_2, y_1, y_2) = 0 \dots \dots \dots (12)$$

$$G(Q_1, Q_2, y_1, y_2) = 0 \dots \dots \dots (13)$$

$$F(Q_2, Q_3, y_2, y_3) = 0 \dots \dots \dots (14)$$

$$G(Q_2, Q_3, y_2, y_3) = 0 \dots \dots \dots (15)$$

Section 4, 5, 6

$$F(Q_4, Q_5, y_4, y_5) = 0 \dots \dots \dots (16)$$

$$G(Q_4, Q_5, y_4, y_5) = 0 \dots \dots \dots (17)$$

$$F(Q_5, Q_6, y_5, y_6) = 0 \dots \dots \dots (18)$$

$$G(Q_5, Q_6, y_5, y_6) = 0 \dots \dots \dots (19)$$

Section 7, 8, 9

$$F(Q_7, Q_8, y_7, y_8) = 0 \dots \dots \dots (20)$$

$$G(Q_7, Q_8, y_7, y_8) = 0 \dots \dots \dots (21)$$

$$F(Q_8, Q_9, y_8, y_9) = 0 \dots \dots \dots (22)$$

$$G(Q_8, Q_9, y_8, y_9) = 0 \dots \dots \dots (23)$$

Section 10, 11, 12

$$F(Q_{10}, Q_{11}, y_{10}, y_{11}) = 0 \dots \dots \dots (24)$$

$$G(Q_{10}, Q_{11}, y_{10}, y_{11}) = 0 \dots \dots \dots (25)$$

$$F(Q_{11}, Q_{12}, y_{11}, y_{12}) = 0 \dots \dots \dots (26)$$

$$G(Q_{11}, Q_{12}, y_{11}, y_{12}) = 0 \dots \dots \dots (27)$$

Section 13, 14

$$F(Q_{13}, Q_{14}, y_{13}, y_{14}) = 0 \dots \dots \dots (28)$$

$$G(Q_{13}, Q_{14}, y_{13}, y_{14}) = 0 \dots \dots \dots (29)$$

This system consists of 18 equations and 28 unknowns. To find a solution ten additional equations are required. They may be written based on the conditions existing at the boundaries.

At each junction the energy level is the same, so that the energy, represented as $y + z + \frac{v^2}{2g}$, can be equated for each section at a junction. Abbreviating the energy equation as

$$H(Q_i, Q_{i+1}, y_i, y_{i+1}) = 0 \dots \dots \dots (30)$$

the following four equations can be written:

Junction 3, 6, 7

$$H(Q_3, Q_7, y_3, y_7) = 0 \dots \dots \dots (31)$$

$$H(Q_6, Q_7, y_6, y_7) = 0 \dots \dots \dots (32)$$

Junction 9, 12, 13

$$H(Q_9, Q_{13}, y_9, y_{13}) = 0 \dots \dots \dots (33)$$

$$H(Q_{12}, Q_{13}, y_{12}, y_{13}) = 0 \dots \dots \dots (34)$$

The law of conservation of mass at each junction is used to obtain the following two equations:

Junction 3, 6, 7

$$F(Q_3, Q_6, Q_7) = 0 \dots \dots \dots (35)$$

Junction 9, 12, 13

$$F(Q_9, Q_{12}, Q_{13}) = 0 \dots \dots \dots (36)$$

The water surface elevations provided by the tide gauges provide boundary data for four more equations. They are represented

$$F(y_1) = 0 \dots \dots \dots (37)$$

$$F(y_4) = 0 \dots \dots \dots (38)$$

$$F(y_{10}) = 0 \dots \dots \dots (39)$$

$$F(y_{14}) = 0 \dots \dots \dots (40)$$

The system of Equations 12 through 29 and 30 through 40 provides twenty eight equations and twenty eight unknowns which can be solved by several methods.

Flow Model Input Data

Boundary conditions, bathymetry data, friction coefficient and initial flow rates were used as model input data. The boundary conditions were expressed as water surface elevations as a function of time. The values are listed in Table 1. The channel section parameters of cross sectional area and wetted perimeter are represented by linear algebraic equations as a function of depth y , measured from mean low water. The equations are:

$$A = A_0 + A_1 y \dots \dots \dots (41)$$

$$P = P_0 + P_1 y \dots \dots \dots (42)$$

Table 1. Field Boundary Data.

TIME	*WATER SURFACE ELEVATION			
	STATION 1 (M)	STATION 2 (M)	STATION 3 (M)	STATION 4 (M)
0.0	0.12	0.11	0.09	0.06
0.5	0.03	0.02	0.03	0.00
1.0	0.00	0.00	0.00	0.03
1.5	0.02	0.03	0.02	0.08
2.0	0.09	0.11	0.08	0.14
2.5	0.20	0.20	0.18	0.24
3.0	0.30	0.30	0.29	0.35
3.5	0.42	0.43	0.47	0.49
4.0	0.58	0.55	0.61	0.66
4.5	0.72	0.72	0.75	0.81
5.0	0.85	0.88	0.90	0.98
5.5	1.04	1.04	1.05	1.16
6.0	1.16	1.14	1.13	1.30
6.5	1.28	1.25	1.26	1.43
7.0	1.34	1.31	1.28	1.54
7.5	1.34	1.33	1.30	1.49
8.0	1.28	1.28	1.28	1.43
8.5	1.19	1.19	1.19	1.22
9.0	1.07	1.07	1.07	1.05
9.5	0.96	0.94	0.94	0.93
10.0	0.84	0.84	0.81	0.73
10.5	0.73	0.73	0.67	0.61
11.0	0.61	0.61	0.58	0.49
11.5	0.49	0.49	0.47	0.37
12.0	0.37	0.40	0.37	0.26
12.5	0.24	0.27	0.24	0.18

*Above Mean Low Water

The values of A_0 , A_1 , P_0 , P_1 are listed for each station in Table 2. The area coefficients were obtained from the fathometer profiles. Since the channels were wide with respect to their depth, the wetted perimeter was considered to be the channel width. The friction coefficient was estimated and then adjusted until the computed results matched the observed values. The initial flow rates were considered for time zero using the current velocities measured with the current meter. Time zero was the predicted time of low tide. The values are listed in Table 3.

Table 2. Coefficients of Expression for Area and Wetted Perimeter.

STATION	COEFFICIENTS FOR AREA		COEFFICIENTS FOR WETTED PERIMETER	
	A_0	A_1	A_0	P_1
1	330.07	175.41	155.45	20.83
2	388.32	206.37	182.88	20.83
3	388.32	206.37	211.35	2.00
4	410.62	128.59	118.87	22.92
5	451.68	141.45	150.40	2.00
6	451.68	141.45	150.40	2.00
7	650.30	346.07	394.25	2.00
8	650.30	346.07	353.57	29.17
9	650.30	346.07	394.25	2.00
10	47.38	187.83	51.82	177.09
11	55.74	220.98	60.96	208.34
12	55.74	220.98	60.96	2.00
13	869.54	366.71	369.84	2.00
14	869.54	366.71	332.22	27.08

$$\text{Cross Sectional Area} = A_0 + A_1 y$$

$$\text{Wetted Perimeter} = P_0 + P_1 y$$

Table 3. Initial Flow Values.

Station	VALUE OF (M)	*CHANNEL BOTTOM ELEV. (M)	**INITIAL DEPTH (M)	INITIAL FLOW RATE (Cu M/S)
1	-650	-4.72	0.12	148
2	-470	-5.03	0.11	148
3	-290	-5.03	0.10	148
4	-520	-5.03	0.12	169
5	-410	-5.03	0.11	169
6	-290	-5.03	0.10	169
7	-290	-4.57	0.10	317
8	-180	-4.11	0.08	3.7
9	0	-4.11	0.07	317
10	-390	-1.52	0.09	39
11	-170	-1.52	0.08	39
12	0	-4.11	0.07	39
13	0	-4.11	0.07	356
14	190	-4.11	0.06	356

*Below Mean Low Water

**Above Mean Low Water

Flow Model Output Data

The output of the model was average discharge and elevation at each station. The computed results for station 14 (See Figure 4) are plotted along with measured data in Figures 5 and 6.

Flow Channels

The bedforms on the offshore bar were analyzed to determine the pattern of flow across the offshore bar. Figure 7 illustrates the ebb flow patterns (larger arrows indicate higher velocities).

SEDIMENT MOVEMENT

Hypothesis of Sediment Bypassing System

Bedform analysis provided the majority of the data used in the formulation of the preliminary hypothesis. Several areas of the inlet were found to carry the majority of the flow as it moved across the offshore bar. The two major areas included an ebb channel, a few meters offshore of Holden Beach, and another minor channel, when compared to the main inlet gorge, near the grid point 2700 (See Figures 4 and 7). These two areas on the offshore bar were found from bedform analysis to carry the highest velocities of flow. A disordered pattern of flow near grid point 2700 was indicated by the observed orientation of the bedforms, but flow over a large portion of the offshore bar tended to move toward the Holden Beach ebb channel. Bedform analysis showed little tendency of the flow to move seaward except through these two previously indicated ebb channels.

Flow data used in the formulation of the preliminary hypothesis included a wave refraction analysis of the area, current velocity measurements, and bathymetry profiles. Wave refraction analysis provided an idea of the location of areas at which extensive erosion would likely occur. The analysis by the Corps of Engineers² found these areas to be the eastern tip of Holden Beach and the western tip of Long Beach. A typical wave from S 60° W and a period of 8 seconds was used in the analysis. The wave refraction analysis also provided the Corps of Engineers with data used to estimate the amount of energy transmitted to the beach zone. From this data, the Corps of Engineers was able to estimate a net annual littoral drift of 245,000 cubic meters/year (320,000 cubic yards/year) in an easterly direction. Current velocity measurements showed the maximum ebb velocity in the inlet gorge to be 1.2 meters/second (4 feet/second) but this velocity was significantly reduced to 0.77 meters/second (2.5 feet/second) in the inlet gorge off Long Beach. This velocity reduction was due to a combination of the widening of the inlet as well as the passing of large volumes of water over the offshore bar. Bathymetry profiles obtained during the period of study showed a maximum depth of 5 meters (17 feet) in the inlet gorge. A depth of 1.5 to 1.8 meters (5 to 6 feet) covered the offshore bar at the high tide. The depth of the water flowing through the ebb channel along Holden Beach reached a depth of 1.5 meters (5 feet) at high tide.

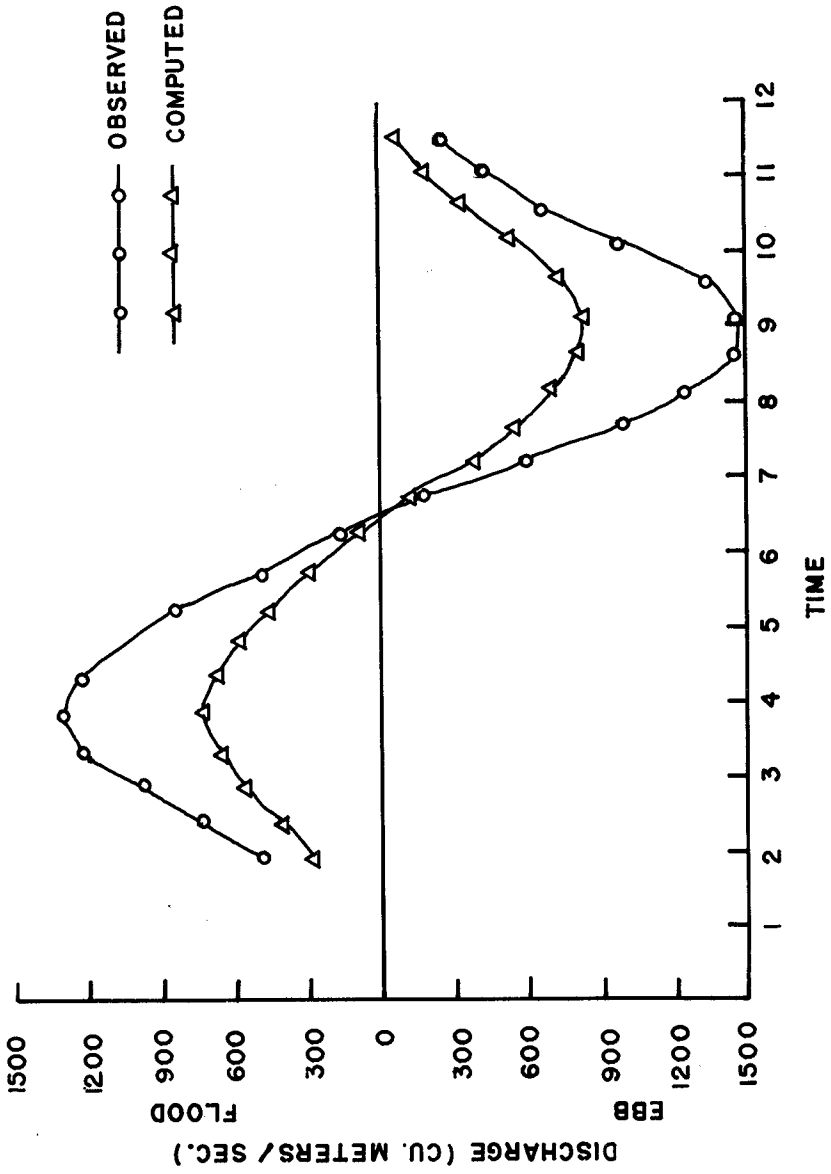


FIGURE 5. Comparison of Computed and Observed Values of Discharge at Station 14.

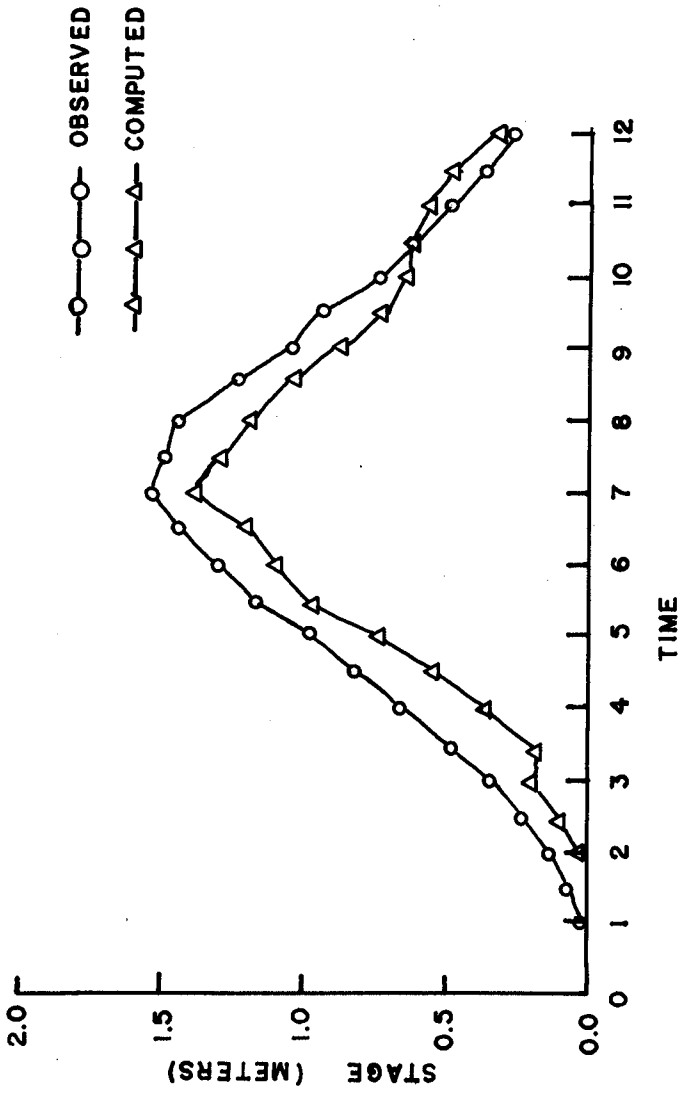


FIGURE 6. Comparison of Computed and Observed Values of Stage at Station 14.

From an analysis of this data, a preliminary hypothesis of the bypassing system was developed. Sediment moved either toward the ebb channel near Holden Beach and was swept into the inlet gorge by the high tidal velocities, or else bypassed the inlet by moving across the offshore bar toward the 2700 grid point. This hypothesis was tested by introducing three different colored tracers onto the offshore bar along the 2000 grid line. Tracer tests were conducted during the ebb to flood cycle in an attempt to verify the pattern of movement indicated from the preliminary hypothesis.

Bar Bypassing Tests

The movement of the sediment across the bar was determined by introducing a fluorescent tracer onto the offshore bar in water soluble bags. The water soluble bags released the tracer onto the bar without allowing it to go into suspension in the water column. Signal green and fire orange were released on the offshore bar along grid line 2000. Blaze orange was raked into the beach between low and high tides along grid line 2000.

Core samples were taken during the tidal cycle. The samples were later analyzed by counting the number of tracer grains present in each sample under a long wave ultraviolet light. Samples containing 1-5 grains were considered to indicate a presence of tracer, while those with 6-10 grains indicated a low concentration; 11-20 grains indicated a medium concentration, and a sample containing more than 20 grains was considered to be highly concentrated. Eighty three core samples taken from the offshore bar were analyzed. Fifty percent of the core samples contained 5 or less grains. Six percent of the core samples did not contain any tracer sand, while twenty-two percent contained 20 or more grains.

Sediment Movement Tests

Ebb to Flood Tests. Two hundred twenty seven kilograms (500 lbs.) of signal green and fire orange tracer were released onto the offshore bar along grid line 2000. Blaze orange was raked onto the beach. The tracer sand entered the bar migration pattern. Samples were taken in the grid system between grid lines 2000 and 3000. Tracer was detected in high concentrations near the point of introduction. The tracer pattern was distinguishable along the shoreline of Holden Beach until it reached the Atlantic Intracoastal Waterway. Signal green tracer initially was stagnate at the end of the ebb channel. Within 24 hours the signal green tracer had established a pattern of movement across the bar. Fire orange tracer established two bypassing patterns; one similar to that which blaze orange initially followed, and the other a pattern of movement also across the offshore bar. Fire orange tracer traveled along the Holden Beach shoreline in an easterly direction until being influenced by the tidal currents of the gorge. From tracer analysis, fire orange tracer was found in detectable concentrations on Long Beach, possibly carried by the current of the inlet gorge. From tracer analysis, fire orange tracer was found in detectable concentrations on Long Beach after 24 hours. A second pattern across the offshore bar was established

as was the case with the blaze orange and signal green tracer. Two types of sediment bypassing were evident at the inlet. The first type tidal flow bypassing, was verified by the pattern of movement of fire orange tracer. The fire orange tracer moved across the offshore bar until being influenced by the tidal currents. The second type found at the inlet was bar bypassing, which from stability analysis was found to be the dominant type of bypassing in effect at the inlet.

Transport Rates Across The Offshore Bar

The transport rates were estimated from the tracer data. The actual transport rates were possible higher than the rates estimated. Blaze orange tracer was first detected at the 2600 grid line (considered to be the edge of the bar) 9 hours after its introduction onto the beach. The rate of transport across the offshore bar was estimated to be 1.8 cm.sec./ (0.059 ft./sec.). Neither signal green nor fire orange tracer was detected on the edge of the bar until 24 hours following introduction. The rate of transport for both tracers was computed to be 0.7 cm./sec.). (0.023 ft./sec.). A composite of the locations of the sediment tracer materials in the bar bypassing tests are shown in Figure 8.

CONCLUSIONS

The following conclusions were drawn from the study:

1. The numerical simulation model agreed reasonably well with the measured values for stage and discharge.
2. The sediment movement patterns in the inlet were related to tidal current patterns.
3. Sediment crossed the inlet from east to west.
4. The offshore bar will continue to grow as it traps and bypasses sand.
5. The inner shoal will continue to grow and encroach on the intracoastal waterway, thus necessitating periodic dredging.

ACKNOWLEDGEMENT

This study was partly supported by the North Carolina Coastal Research Program and by the Center for Marine and Coastal Studies.

LIST OF REFERENCES

1. Amein, M., "Computation of Flow Through Masonboro Inlet, N. C.", Sea Grant Publication UNC-SG-73-15, Sea Grant Program, N. C. State University, Raleigh, North Carolina, 1973, pp. 7-35.
2. U. S. Army Corps of Engineers, Wilmington District, General Design Memorandum, Phase I, Hurricane Wave Protection Beach Erosion Control Brunswick County, North Carolina, Beach Projects-Yaupon Beach and Long Beach Segments, July 1973.

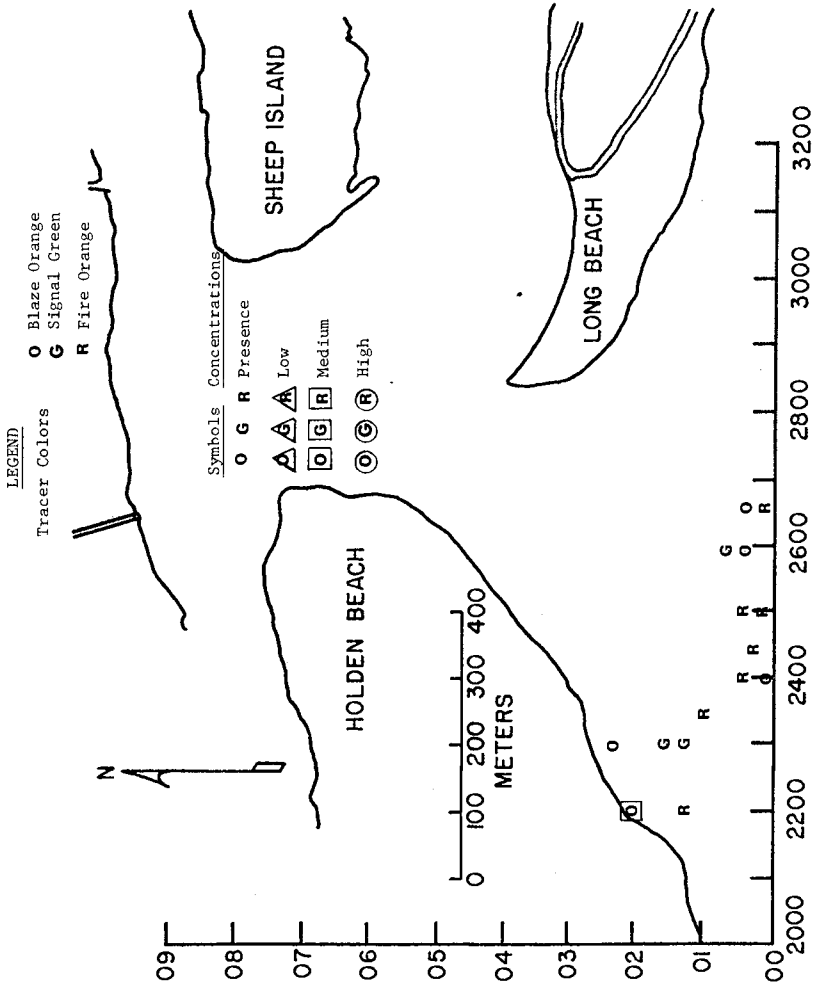


FIGURE 8. Location of Detected Blaze Orange, Signal Green, Fire Orange Trace Sand - AM, 25 August 1974. Note: 24 Hours After Introduction.